scientific reports

Check for updates

OPEN

# Controlling synchronization of gamma oscillations by astrocytic modulation in a model hippocampal neural network

Sergey Makovkin[1]✉, Evgeny Kozinov[2], Mikhail Ivanchenko[1] & Susanna Gordleeva[3,4,5]✉

**Recent in vitro and in vivo experiments demonstrate that astrocytes participate in the maintenance of cortical gamma oscillations and recognition memory. However, the mathematical understanding of the underlying dynamical mechanisms remains largely incomplete. Here we investigate how the interplay of slow modulatory astrocytic signaling with fast synaptic transmission controls coherent oscillations in the network of hippocampal interneurons that receive inputs from pyramidal cells. We show that the astrocytic regulation of signal transmission between neurons improves the firing synchrony and extends the region of coherent oscillations in the biologically relevant values of synaptic conductance. Astrocyte-mediated potentiation of inhibitory synaptic transmission markedly enhances the coherence of network oscillations over a broad range of model parameters. Astrocytic regulation of excitatory synaptic input improves the robustness of interneuron network gamma oscillations induced by physiologically relevant excitatory model drive. These findings suggest a mechanism, by which the astrocytes become involved in cognitive function and information processing through modulating fast neural network dynamics.**

Synchronous rhythms of the brain support a variety of cognitive functions by providing temporal and spatial coordination of neural network signaling[1,2]. Particularly, fast gamma cortical oscillations ($\gamma$ 20–80 Hz) have been recorded in many cortical brain structures during both waking and sleep states. They are commonly associated with sensory processes[3], attention[4], learning, memory storage, and retrieval[5,6]. Nonetheless, functions of $\gamma$ oscillations, their cellular and network mechanisms remain a matter of debate[7]. Experimental and theoretical evidence suggests that the generation of $\gamma$ network oscillations critically depends on the rhythmic activity of local networks of synaptically connected GABAergic interneurons, which synchronize spikes in pyramidal neurons[8–12]. Although the key contribution of interneurons to $\gamma$ rhythm formation has been well established, the mechanisms underlying the generation of coherent oscillations in the interneuron networks have not been fully clarified yet.

Following the experimental findings, which show that interneurons, in particular fast-spiking basket cells (BCs), can generate $\gamma$ activity in vitro[8,10] and in vivo[13,14], numerous computational studies proposed mechanisms of synchrony emergence in a recurrent network of interneurons in response to a tonic excitatory drive[11,15–18]. A major challenge of interneuron network models is understanding the mechanisms of the robustness of gamma oscillations against heterogeneity in the excitatory drive (for review, see[19]). Existing models with slow, weak, and hyperpolarizing synapses generate synchronized gamma activity only when the heterogeneity of the input drive is low and the amplitude is high[11], which is physiologically inconsistent[20,21]. It was shown that sensitivity to heterogeneity can be significantly reduced by incorporating realistic synaptic properties in the models[12,15,22]. Search for the biologically plausible mechanisms to improve the robustness of coherent oscillation formation in the interneuron network models against heterogeneity remains a highly relevant task.

[1]Department of Applied Mathematics, Institute of Information Technology, Mathematics and Mechanics, Lobachevsky University, 23, Gagarin Ave., Nizhny Novgorod 603022, Russia. [2]Department of Supercomputer Computation, Institute of Information Technology, Mathematics and Mechanics, Lobachevsky University, 23, Gagarin Ave., Nizhny Novgorod 603022, Russia. [3]Neurotechnology Department, Institute of Biology and Biomedicine, Lobachevsky University, 23, Gagarin Ave., Nizhny Novgorod 603022, Russia. [4]Neuroscience and Cognitive Technology Laboratory, Center for Technologies in Robotics and Mechatronics Components, Innopolis University, 1, Universitetskaya Str., Innopolis 420500, Russia. [5]Center for Neurotechnology and Machine Learning, Immanuel Kant Baltic Federal University, 14, Nevskogo Str., Kaliningrad 236041, Russia. ✉email: makovkin@neuro.nnov.ru; gordleeva@neuro.nnov.ru

Recently, it was shown that glial cells substantially influence the formation of gamma oscillatory rhythms, which were previously thought to be a product of neuronal activity[23–25]. In particular, it was revealed that astrocytic vesicular release is necessary to maintain functional gamma oscillations, and it is essential for novel object recognition behavior both in vitro and in awake-behaving animals[23]. However, the cellular and network mechanisms underlying astrocytic involvement in the formation of synchronized neural network $\gamma$ activity remain undefined.

Astrocytes sense and integrate neuronal activity by responding with intracellular $Ca^{2+}$ elevations[26]. Due to the fact that astrocytic calcium dynamics has a significantly slower timescale than the fast synaptic transmission of neurons, it has been assumed for decades that astrocytes do not play a major role in modulating neural network activity, neural information processing, and cognition. Nevertheless, recent studies have shown that astrocytes can regulate neuronal excitability, synaptic transmission, and plasticity[27,28] through the release of chemical transmitters (termed "gliotransmitters") induced by intracellular $Ca^{2+}$ signals. Although these findings have been independently confirmed by several groups, the functional significance and properties of gliotransmission remain a matter of debate[29,30]. Numerous studies reveal the unexpected role of astrocytes in the coordination of the fast dynamics of neural circuits that underlie normal cognitive behaviors[31–33]. Several computational studies discuss the role of astrocytes in the spatio-temporal coordination of neural network signaling[34–39], the emergence of coherent oscillations[40,41], information processing[42–46], and memory formation[47–51]. Savtchenko and Rusakov showed that the astroglia-like, volume-limited synaptic regulation of excitatory input appears to be better at preserving interneuron network synchronization while inducing the network clustering to neuron subgroups with distinct firing patterns[41].

Nonetheless, the way the interplay of slow modulatory astrocytic signaling with fast synaptic transmission is involved in the formation of coherent oscillations in the interneuron network remains an open question. To address this issue, we studied the role of astrocyte-mediated regulation of synaptic transmission in the generation of $\gamma$ interneuron network oscillations. In particular, we investigated the computational model of hippocampal interneuron network which displays physiologically plausible oscillatory behaviors[11,12,17]. To do that we complemented it with an astrocytic network and explored how $\gamma$ oscillations in the interneuron network can be regulated by the astrocytic modulation of synaptic transmission.

## Methods

In our previous work, we investigated the dynamics of the bidirectional neuron-astrocyte interaction in a minimal network model[36]. We showed that astrocytes can induce the intermittent synchronization of a pair of synaptically coupled fast spiking neurons on the slow timescale of calcium oscillations. Here, we employ a similar approach to study the dynamics of an extended version of the model .

We studied the interneuron network model of 200 neurons arranged on a virtual ring[15], which mimicked the organization of the BC network in hippocampal area CA1. Each neuron was randomly connected to its 100 nearest neighbors by inhibitory chemical synapses with a probability of 0.5. This connectivity reflects anatomical analyses of functional links among interneurons in area CA1[52]. Interneurons receive excitatory inputs from pyramidal neurons whose stochastic firing is triggered by the random Poisson spike trains with a given rate. Astrocytes are organized in a ring-shaped network repeating the topology of the interneuron network. It was shown that the number of astrocytes and neurons is approximately the same in the mammalian brain and that the individual astrocytes occupy separate, non-overlapping tissue domains[53]. The astrocytic network in the proposed model consists of 200 diffusely coupled astrocytes. Each astrocyte is connected to the two nearest neighboring astrocytes through gap junctions[54]. Astrocytes generate the elevations of intracellular $Ca^{2+}$ in response to a synaptically released neurotransmitter (glutamate) from the pyramidal neurons. Such $Ca^{2+}$ activity can regulate the strength of synaptic connections of near and distant tripartite synapses at diverse timescales through gliotransmitter release[27]. It was shown that locations of dendritic trees of the BCs in the hippocampus do not significantly overlap with each other[55]. Therefore, an individual astrocyte can influence only one or a small proportion of BCs from the entire network[41]. The architecture of the simulated neuron-astrocyte network is shown in Fig. 1. Each astrocyte is coupled to one corresponding interneuron and acts by modulating incoming connections of the neuron from interneurons or from pyramidal neuron. In this paper, we studied two types of astrocytic modulations of signal transmission in the interneuron network. In particular, we considered astrocyte-induced modulation of (i) inhibitory synaptic transmission in an interneuron network (Fig. 1b) and (ii) excitatory synaptic transmission from pyramidal neurons to interneurons (Fig. 1c).

**Neural network.** Various models describe the neuronal spiking dynamics at different levels of bio-fidelity, from simplified leaky integrate-and-fire model to biophysical Hodgkin-Huxley equations[56]. Here we use the Mainen modification of the Hodgkin-Huxley neuron model for the mammalian brain[57,58], as the most biologically plausible. Membrane potential neuronal dynamics was modeled as

$$\begin{cases} \dfrac{dV_i}{dt} = \dfrac{1}{C}\left(I_{channel\,i} + I_{app} + I_{P\,i} + I_{syn_i}\right), \\ \dfrac{dx_i}{dt} = \alpha_x(1-x_i) - \beta_x x_i,\ x = m,n,h; \\ I_{channel\,i} = g_{Na} m_i^3 h_i (E_{Na} - V_i) + g_K n_i (E_K - V_i) + g_{Leak}(E_{Leak} - V_i), \end{cases} \tag{1}$$

where $i$ ($i = 1, \ldots, 200$) corresponds to a neuronal index, the transmembrane potential $V$ is given in mV, and time $t$ in ms. $I_{channel}$ is the sum of the transmembrane ionic currents (i.e., sodium, potassium, and leak currents).

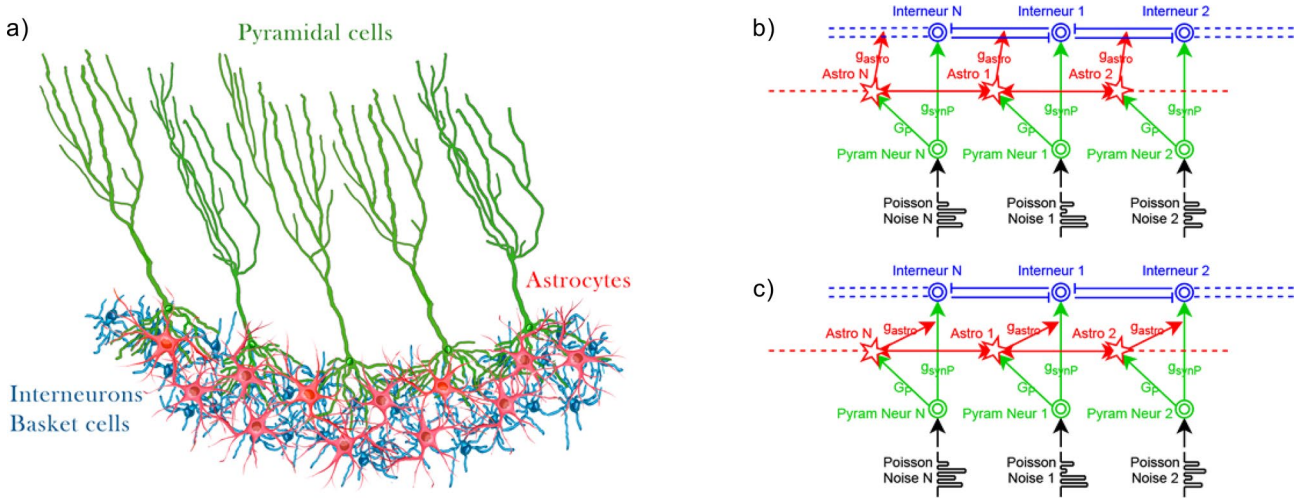


**Figure 1.** (**a**) A scheme illustrating the organization of modeled BCs-pyramidal cells-astrocytes network in hippocampal area CA1[55]. (**b**,**c**) Architecture of the neuron-astrocyte network model. The interneuron network model consists of 200 neurons arranged on a virtual ring[15], which mimics the organization of the basket cell network. Each neuron is randomly connected to its 100 nearest neighbors by inhibitory chemical synapses with a probability of 0.5. Interneurons receive excitatory inputs from pyramidal neurons whose stochastic firing is triggered by the random Poisson spike trains. Astrocytes are organized in a ring-shaped network repeating the topology of the interneuron network. Each astrocyte in the proposed model is connected to the neighboring astrocytes through gap junctions. Two types of astrocytic influence on signal transmission in the neuronal network are considered: astrocyte-induced modulation of (**b**) inhibitory synaptic transmission in the interneuron network and (**c**) excitatory synaptic transmission from pyramidal neurons to interneurons.

Nonlinear functions $\alpha_x$ and $\beta_x$ for gating variables are taken from the Mainen modification of the Hodgkin–Huxley model[57,58]:

$$\begin{aligned}
\alpha_m &= \frac{0.182(V_i+35)}{1-e^{\frac{-(V_i+35)}{9}}}; \quad \beta_m = \frac{-0.124(V_i+35)}{1-e^{\frac{(V_i+35)}{9}}}; \\
\alpha_n &= \frac{0.02(V_i-25)}{1-e^{\frac{-(V_i-25)}{9}}}; \quad \beta_n = \frac{-0.002(V_i-25)}{1-e^{\frac{(V_i-25)}{9}}}; \\
\alpha_h &= 0.25e^{\frac{-(V_i+90)}{12}}; \quad \beta_h = 0.25\frac{e^{\frac{V_i+62}{6}}}{e^{\frac{V_i+90}{12}}}.
\end{aligned} \tag{2}$$

Throughout this paper, we use the following parameter values: $C = 1\ \mu\text{F/cm}^2$; $g_{Na} = 40\ \text{mS/cm}^2$; $g_K = 35\ \text{mS/cm}^2$; $g_{Leak} = 0.3\ \text{mS/cm}^2$; $E_{Na} = 55\ \text{mV}$; $E_K = -77\ \text{mV}$; $E_{Leak} = -54.4\ \text{mV}$. The constant applied current $I_{app}$ defines the dynamical regime (oscillatory, bistable, or excitable) of a neuron[59,60]. We chose the rest mode of a neuron with an equilibrium state of steady focus with a shift current value $I_{app} = 0.7\ \mu\text{A/cm}^2$[36].

Each pyramidal neuron receives an external input $I_P$ defined as a Poisson pulse train with mean rate $F_{in}$ of 0–400 Hz chosen in accordance with earlier estimates[41]. The pulse has a rectangular shape with a constant duration of 2 ms, and amplitudes sampled independently from a uniform distribution in $[0.0;\ 2.5]\ \mu\text{A/cm}^2$. Each pulse train is generated independently for each neuron. For interneurons $I_P = 0$.

The total synaptic current $I_{syn}$ received by neuron $i$ from $N$ presynaptic neurons is defined as[42,59]:

$$\begin{aligned}
I_{syn_i} &= \sum_j^N \frac{\tilde{g}_{syn}(V_i - E_{syn_j})}{1+e^{\frac{-V_j}{k_{syn}}}}; \\
\tilde{g}_{syn} &= \begin{cases} g_{syn}(1+g_{astro}[Ca^{2+}]_i), & \text{if } [Ca^{2+}]_i \geq 0.3\ \mu\text{M}, \\ g_{syn}, & \text{otherwise} \end{cases}
\end{aligned} \tag{3}$$

where $j$ denotes a presynaptic neuronal index, the reversal potential is $E_{syn} = -90$ mV for the inhibitory synapse and $E_{syn} = 0$ mV for the excitatory one, $k_{syn} = 0.2$ mV. Parameter $\tilde{g}_{syn}$ corresponds to the synaptic weight and incorporates the astrocyte modulation due to the release of gliotransmitters in the tripartite synapses. To describe the astrocytic impact in synaptic transmission, we use a simplified approach tested in our previous studies[36,42,44]. We assume that upon reaching the intracellular calcium concentration, $[Ca^{2+}]$, the threshold in 0.3 μM, astrocytes release the gliotransmitters to the synaptic cleft whose interaction with pre- and postsynaptic terminals regulates the strength of the synaptic connections. Parameter $g_{syn}$ is the baseline synaptic weight in neuron-neuron communication (we use $g_{syn}$ to denote the synaptic weight between interneurons and $g_{synP}$ for the synaptic weight between pyramidal neurons and interneurons). Parameter $g_{astro}$ is the strength of the astrocyte-induced modulation of the synaptic weight.

**Astrocytic network.** Each astrocyte tracks the activity of pyramidal neurons and can generate the elevation of the intracellular concentration of $IP_3$ followed by the emergence of calcium pulse in response to changes in neurotransmitter (glutamate) concentration in the synaptic cleft. When the pyramidal neuron $i$ generates an action potential, it causes the release of glutamate from the synapse. The glutamate concentration is described by the following equation[36,44,61]:

$$\frac{dG_i}{dt} = -\alpha_G G_i + \beta_G \frac{1}{1 + e^{(-\frac{V_i}{0.5})}}, \tag{4}$$

where $\alpha_G = 25\ s^{-1}$ and $\beta_G = 500\ s^{-1}$ denote the relaxation and production rates of glutamate. Glutamate binds to the metabotropic glutamate receptors on the astrocytic membrane, which is located close to the synapse and activates $IP_3$ signaling in the astrocyte. The dynamics of the intracellular concentration of $IP_3$ in astrocytes is expressed as follows[62]:

$$\begin{aligned} &\frac{dIP3_i}{dt} = \frac{IP3^* - IP3_i}{\tau_{IP3}} + J_{PLC\,i} + J_{IP3\,diff\,i} + J_{Glu\,i}, \\ &J_{PLC\,i} = v_4\big([Ca^{2+}]_i + (1-\alpha)k_4\big)/([Ca^{2+}]_i + k_4), \\ &J_{IP3\,diff\,i} = d_{IP3}(IP3_{i-1} + IP3_{i+1} - 2IP3_i); \end{aligned} \tag{5}$$

where the parameter $IP3^*$ is the steady-state intracellular concentration of $IP_3$, currents $J_{PLC}$, $J_{IP3\,diff}$ denote the $IP_3$ production caused by the activation of PLC by the calcium released from the endoplasmic reticulum, and the $IP_3$ diffusion between neighboring cells through the gap junctions, respectively. The current $J_{Glu}$ describes the glutamate-induced production of the $IP_3$ in response to neuronal activity and is modeled as[36,44]

$$J_{Glu\,i} = \frac{\alpha_{Glu}}{1 + e^{\frac{-(G_i - 0.25)}{0.01}}}. \tag{6}$$

Glutamate released from presynaptic neurons is integrated over a larger timescale by the $IP_3$ dynamics through $J_{Glu}$. An increase in cytosolic $IP_3$ induces the opening of the $Ca^{2+}$-dependent receptors at the endoplasmic reticulum (ER), which results in a $Ca^{2+}$ influx from ER to the cytosolic volume. This process is known as calcium-induced calcium release (CICR) and can be described by the widely used biophysical model for astrocytic dynamics[62]:

$$\begin{cases} \dfrac{d[Ca^{2+}]_i}{dt} = J_{ER\,i} - J_{pump\,i} + J_{leak\,i} + J_{in\,i} - J_{out\,i} + J_{Ca\,diff\,i}, \\ \dfrac{dz_i}{dt} = a_2\left(d_2\dfrac{IP3_i + d_1}{IP3_i + d_3}(1 - z_i) - [Ca^{2+}]_i z_i\right), \end{cases} \tag{7}$$

where $[Ca^{2+}]$ is the intracellular concentration of $Ca^{2+}$, and $z$ is the fraction of $IP_3$ receptors that have not been inactivated by $Ca^{2+}$. $J_{ER}$, $J_{pump}$, $J_{leak}$ denote the fluxes from ER to the cytosol by the joint gating of $Ca^{2+}$ and $IP_3$, via the ATP-dependent pump from the cytosol to the ER, and the leaked flux from the ER to the cytosol, respectively. Calcium exchange with the extracellular space is described by $J_{in}$ and $J_{out}$. The flux $J_{Ca\,diff}$ is the diffusive flux of $Ca^{2+}$ between astrocytes via gap junctions[63]. They evolve according to the following equations[62]:

$$\begin{aligned} &J_{ER\,i} = c_1 v_1 IP3_i^3 [Ca^{2+}]_i^3 z_i^3 \left(\frac{c_0}{c_1} - (1 + \frac{1}{c_1})[Ca^{2+}]_i\right) / \left[(IP3_i + d_1)([Ca^{2+}]_i + d_5)\right]^3; \\ &J_{pump\,i} = v_3 [Ca^{2+}]_i^2 / (k_3^2 + [Ca^{2+}]_i^2); \\ &J_{leak\,i} = c_1 v_2 \left(\frac{c_0}{c_1} - (1 + \frac{1}{c_1})[Ca^{2+}]_i\right); \\ &J_{in\,i} = v_5 + v_6 IP3_i^2 / (k_2^2 + IP3_i^2); \\ &J_{out\,i} = k_1 [Ca^{2+}]_i; \\ &J_{Ca\,diff\,i} = d_{Ca}([Ca^{2+}]_{i-1} + [Ca^{2+}]_{i+1} - 2[Ca^{2+}]_i). \end{aligned} \tag{8}$$

Biophysical meaning of all parameters in Eqs. (5–8) and their experimentally determined values can be found in[62,64]. For our purposes, we fix $c_0 = 2\ \mu M; c_1 = 0.185; v_1 = 6\ s^{-1}; v_2 = 0.11\ s^{-1}; v_3 = 2.2\ \mu M/s; v_4 = 0.3\ \mu M/s; v_5 = 0.025\ \mu M/s;\ v_6 = 0.2\ \mu M/s;\ k_1 = 0.5\ s^{-1};\ k_2 = 1\ \mu M;\ k_3 = 0.1;\ k_4 = 1.1\ \mu M/s;\ a_2 = 0.14\ \mu M/s; d_1 = 0.13\ \mu M; d_2 = 1.049\ \mu M; d_3 = 0.9434\ \mu M; d_5 = 0.082\ \mu M; \alpha = 0.8; \tau_{IP3} = 7.143\ s; IP3^* = 0.16\ \mu M; d_{Ca} = 0.001\ s^{-1}; d_{IP3} = 0.12\ s^{-1}; \alpha_{Glu} = 2$. We rescale the time units of the astrocyte model in order to match it in milliseconds for numerical integration.

**Numerical methods.** Simulations were done using a finite difference integration scheme based on the fourth-order Runge-Kutta algorithm with time step $\Delta t = 5 \cdot 10^{-3}$ ms. The total simulation time was 180 s. Network signaling was analyzed in the time interval from 15 to 180 s. Initial conditions used for simulation can be found in Appendix A (Supplementary Information).

**A measure of network coherence.** Frequency and coherence of interneuron network activity were determined in 500-ms epochs. Average firing frequency, Ω, was determined as the inverse of the mean interspike interval. Neuronal membrane potentials were binarized (0—no action potential, 1—action potentials were generated in a given time interval). The network coherence was calculated as the mean of the coherence in all pairs of interneurons in the time window $\tau = 0.1/\Omega$, $k(\tau)$, and was defined as the following[11,12]:

$$k_{i,j}(\tau) = \frac{\sum_{l=1}^{L} X(l)Y(l)}{\sqrt{\sum_{l=1}^{L} X(l) \sum_{l=1}^{L} Y(l)}}, \tag{9}$$

where $i$ and $j$ denote the two interneurons, $X(l)$ and $Y(l)$ are the binary action potential patterns, and $L$ is the number of time bins. In the case of full synchrony, $k(\tau)$ is 1 for all nonzero $\tau$ values; whereas in the case of total asynchrony, $k(\tau)$ becomes a linearly increasing function of $\tau$. To measure the network coherence in the course of astrocyte-mediated modulation of synaptic transmission, $k_{astro}$, we calculate the extrema of the coherence, $k$, during the $Ca^{2+}$ elevations in astrocytes ($[Ca^{2+}] > 0.3$ μM), $k_{astro_i}$, and then average them over all calcium pulses in the simulation.

## Results

In situ and in vivo experimental studies reveal a rich diversity of physiological consequences of astrocyte-mediated neuromodulation[27]. Involved in the same neuronal circuit astrocytes can release various types of gliotransmitters that can modulate synaptic transmission in different ways. For instance, in the hippocampus, the astroglial release of glutamate can potentiate inhibitory transmission by triggering presynaptic kainate receptors[65] and support neuronal synchrony by triggering postsynaptic NMDARs[66]. In the hippocampal CA1 region, the gliotransmitter ATP can also depress or enhance excitatory synaptic transmission by triggering either A1 or A2 receptors, respectively[67,68]. To mimic multiple forms of astrocytic physiological actions on synaptic transmission in the modeled network, we explored two scenarios of neuron-astrocyte interaction with variable gliotransmitter-induced changes in synaptic transmission. We explored how synchrony in an interneuron network can be regulated by the astrocytic influence (i) on inhibitory transmission in the interneuron network (Fig. 1a), and (ii) on excitatory synaptic inputs from pyramidal neurons to interneurons (Fig. 1b).

The dynamics of interneuron network model used in this study has been investigated in numerous previous studies[9,11,12,17]. In this study, we focused on the variation of two parameters of the astrocyte-induced regulatory action: the direction and the magnitude of the synaptic change. Without the astrocytes, an interneuron network in default conditions[11,12,17] displays coherent fast oscillations with $k = 0.5$ and the frequency of 21 Hz (Fig. 2a,b) which corresponds to the lower bound of the gamma-frequency range observed in the hippocampal interneuronal networks during behavioral arousal[11]. The interneuronal activity was induced by the stochastic excitatory synaptic inputs from pyramidal neurons driven by Poisson trains with a given frequency, $F_{in}$, chosen in accordance with earlier estimates. The emergence of interneuron synchronization and network coherence estimated by $k$ is critically dependent on the frequency of excitatory inputs ($F_{in}$) and the unitary inhibitory synaptic weight ($g_{syn}$). We analyzed the dependence of coherence level in the interneuron network signaling on $g_{syn}$ and $F_{in}$ (Fig. 2c). In the selected range of parameter values, the network synchrony is realized when $F_{in}$ is larger than the critical value $F_{in\ min}$, which is required for signal transmission from pyramidal neurons to interneurons. $F_{in\ min}$ nonlinearly decreases with the enhancement of inhibitory synapses till $g_{syn} \approx 0.01$ mS/cm$^2$. The coherence of interneuron network oscillations increases with synaptic strength.

**Influence of the astrocytic modulation of the inhibitory synaptic transmission on γ oscillations in the interneuron network.** We further explored the impact of the astrocytic modulation of synaptic transmission between interneurons on the coherence ($k$) of network oscillations. Two cases were considered: astrocyte-induced depression and potentiation of inhibitory transmission. Spiking activity of pyramidal neurons leads to the emergence of the calcium oscillations in astrocytes, which originally remained in the steady state (Fig. 3a,f). The dynamics of $\gamma$ rhythm modulation mediated by astrocytes is shown in Fig. 3. During astrocytic facilitation of the inhibitory synapses, the network oscillated with markedly increased coherence (Fig. 3g–j), while astrocyte-induced depression of coupling between interneurons induces coherence decrease (Fig. 3b–e).

To investigate the phenomenon in more detail, we explored network oscillations coherence at the intervals of astrocytic modulation (when $[Ca^{2+}] > 0.3$ μM). The maximum (for astrocyte-induced potentiation of inhibitory transmission) or minimum (for astrocyte-induced depression of inhibitory transmission) of the coherence coefficient were calculated ($k_{astro_i}$ on Fig. 3c,h), which were then averaged over all calcium pulses in the simulation. Next, we examined the dependence of the network coherence during astrocyte-mediated modulation, $k_{astro}$, on $g_{syn}$ and $F_{in}$ (Fig. 4a,b) and compared it with the coherence of interneuron activity without astrocytes, $k$ (Fig. 2c).

Astrocyte-induced reduction of synaptic strength results in the decrease of $\gamma$ oscillations coherence in the interneuron network in all considered ranges of parameters $g_{syn}$, $F_{in}$ (Fig. 4a,c). Therefore, reaching a high level ($k > 0.6$) of coherence for considered small values of synaptic weights $g_{syn} < 0.02$ mS/cm$^2$ becomes impossible.

On the contrary, the interneuron network with astrocyte-mediated potentiation of inhibitory transmission oscillates with markedly increased coherence. Such astrocytic impact induces the extension of the high-coherence region and leads to its shift to lower $g_{syn}$ value (0.016 mS/cm$^2$ < $g_{syn}$ < 0.02 mS/cm$^2$ in the absence of astrocytes versus 0.008 mS/cm$^2$ < $g_{syn}$ < 0.02 mS/cm$^2$ for astrocytic enhancement of the synaptic strength (Fig. 4b,d). The astrocytic influence extends the region of coherent oscillations to the range of weaker synaptic conductances, which belong to the experimentally determined postsynaptic conductances range[15]. The parameter dependence

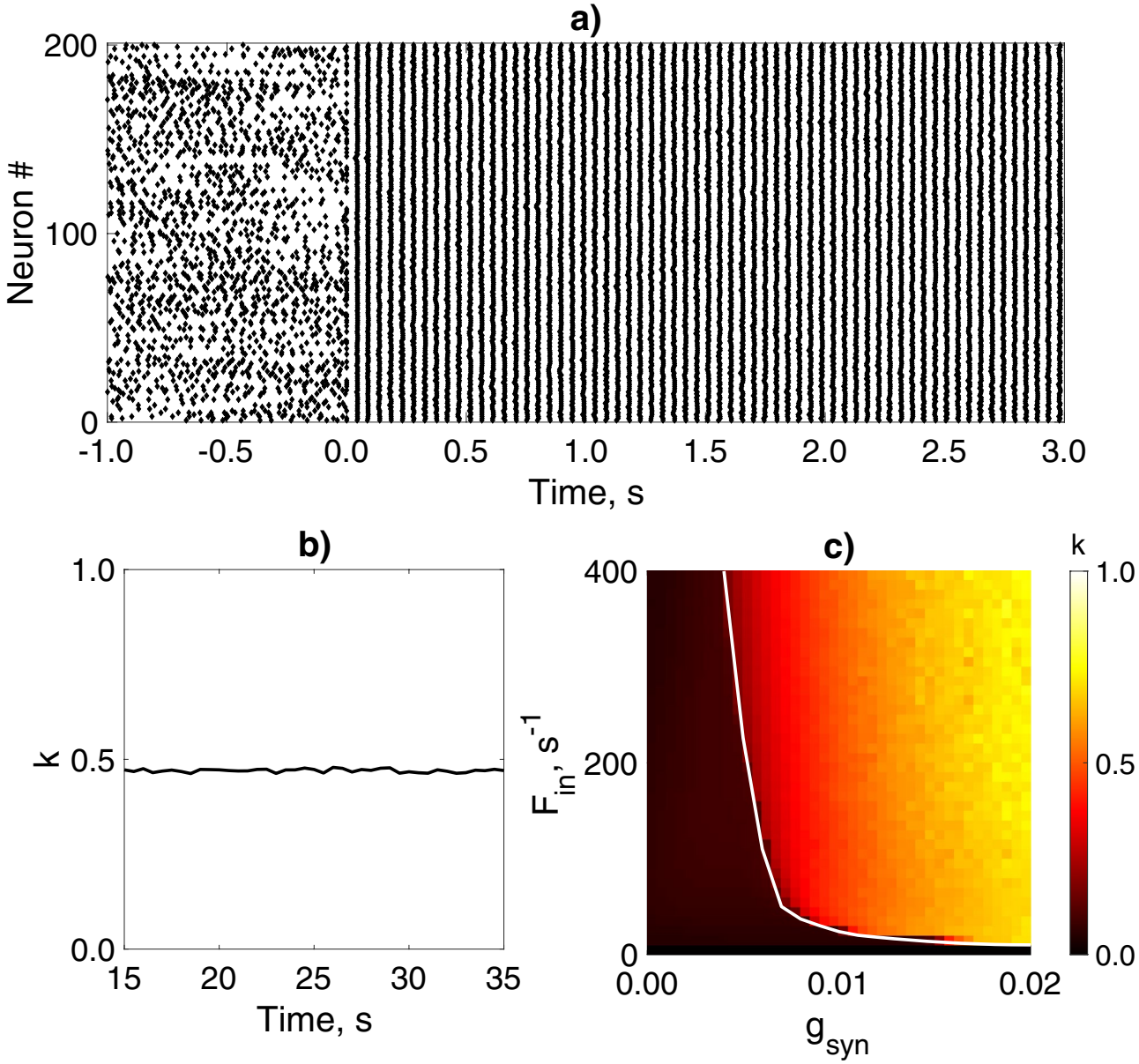


**Figure 2.** $\gamma$ oscillations in the interneuron network model. (**a**) Raster plots of the interneuron network activity with default parameter settings. Synapses were activated at 0 s ($g_{syn} = 0.01$ mS/cm$^2$, $F_{in} = 260$ s$^{-1}$). (**b**) Coherence ($k$) is determined in 500-ms windows for the network oscillations shown on (**a**). (**c**) Mean network coherence ($k$) is plotted against the frequency of excitatory inputs ($F_{in}$) and the synaptic weight between interneurons ($g_{syn}$). The white line corresponds to the border of the synchronization region with $k = 0.4$. Each pixel represents an average of over 10 simulations.

curve ($g_{syn}$, $F_{in}$) determines the occurrence of synchronization shifts to lower values of $g_{syn}$ for the entire range of $F_{in} > F_{in\ min}$ (Fig. 4b,d).

**Influence of the astrocytic modulation of the excitatory synaptic inputs on $\gamma$ oscillations in the interneuron network.** Experimental studies showed that the tonic excitatory input currents in interneurons that induce $\gamma$ oscillations are small and highly heterogeneous[20,21]. However, previous interneuron network models required a highly homogeneous tonic excitatory drive or strong synaptic conductance values to compensate for the increased level of heterogeneity for emergence of synchronized activity[12,15,69]. Search for mechanisms to improve the robustness of generation of highly coherent gamma oscillations in the interneuron network has remained a relevant task for over two decades[17]. We, therefore, investigated how astrocytic modulation of excitatory synaptic drive from pyramidal neurons to interneurons can contribute to $\gamma$ rhythm formation.

In the model, the amplitudes of the excitatory synaptic currents in interneurons are determined by the strength of synaptic transmission between pyramidal neurons and interneurons, $g_{synP}$. In accordance with experimental data[9,17], each pyramidal neuron was activated by Poisson pulse trains at a mean frequency of $F_{in} = 260$ s$^{-1}$ with amplitudes chosen randomly from a uniform distribution within a given range [0.0; 2.5] μA/cm$^2$. Without

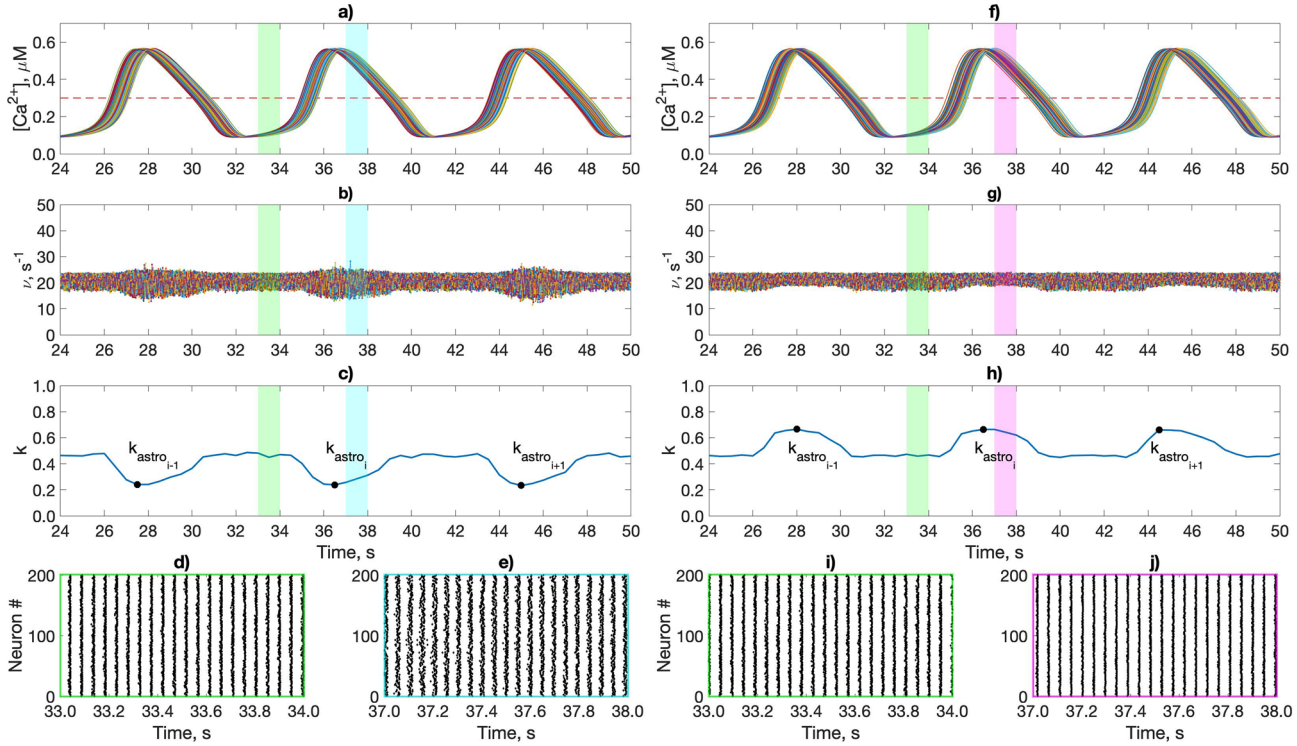


**Figure 3.** The astrocytic calcium dynamics induced by the activity of pyramidal neurons and its influence on $\gamma$ oscillations in the interneuron network through astrocyte-mediated modulation of the inhibitory synaptic weights. (**a**,**f**) The intracellular $Ca^{2+}$ concentration in the astrocytic network. (**b**,**g**) Instantaneous firing rates of interneurons. (**c**,**h**) Coherence network ($k$) dynamics. (**d**,**e**,**i**,**j**) Raster plots of an interneuron network activity. The dotted lines show the threshold $Ca^{2+}$ concentration for the astrocytic modulation of the synapse $[Ca^{2+}]$ = 0.3 μM. Color coding of the 1 second long fragments of network activity: green—without astrocytic influence; blue—astrocyte-mediated depression of the inhibitory synapses ($g_{astro} = -0.8$); magenta—astrocyte-mediated facilitation of the inhibitory synapses ($g_{astro} = 1.2$). An example of used minimum/maximum values of the interneurons coherence during the $Ca^{2+}$ elevations in astrocytes marked with dots $k_{astro}$. $F_{in} = 260\ s^{-1}$; $g_{syn} = 0.009\ mS/cm^2$; $g_{synp} = 0.7\ mS/cm^2$.

astrocytes for a fixed frequency, $F_{in}$, the synchronization emerges only within a specific subregion of the parameter space ($g_{syn}$, $g_{synp}$) (Fig. 5b), which expands as the strength of inhibitory coupling between interneurons, $g_{syn}$ increases. The lower boundary of the coherence region, $g_{synp\ min}$, corresponds to the minimum amplitude of the excitatory drive required for activity generation in interneurons (action-potential threshold). $g_{synp\ min}$ decreases nonlinearly as the interneuron coupling strength rises. The high-coherence ($k > 0.6$) network oscillations almost reaching the threshold values $g_{synp}$ were observed in the model with strong inhibitory connectivity.

Similar to the previous scenario with astrocytic modulation of the inhibitory synaptic transmission, we analyzed the contribution of the gliotransmitter-induced potentiation and depression of the excitatory synapses to the modulation of the interneuron network coherence. The astrocytic suppression of excitatory synaptic drive ($g_{astro} < 0$) evokes the significant network coherence enhancement (Fig. 6a–e). During astrocytic depression of the excitatory synaptic transmission, the high-coherence region expanded considerably, while the entire region of coherence slightly shifted to higher $g_{synp}$ values (Fig. 5a,d). Conversely, when astrocytes facilitated the synaptic drive ($g_{astro} > 0$), the network oscillated with low coherence (Fig. 6f–j). Astrocyte-enhanced amplitudes of the excitatory synaptic currents result in high heterogeneity of the intrinsic firing rates of individual interneurons. Thus, the global network synchrony maintenance requires stronger connectivity between interneurons (Fig. 5c,e).

Next, we analyzed the dependence of coherence on the astrocytic modulation ($g_{astro}$) and the excitatory synaptic strength ($g_{synp}$). Two values of interneuronal connectivity ($g_{syn}$) were compared, 0.01 $mS/cm^2$ corresponded to medium coherence with $k \leqslant 0.5$, and 0.017 $mS/cm^2$ corresponded to high coherence with $k \geqslant 0.5$ (Fig. 7a,c). We also examined how the $g_{synp}$ range corresponding to different coherence levels depends on the astrocytic modulation strength, $g_{astro}$ (Fig. 7b,d).

Astrocytic depression gain leads to considerable extension of $g_{synp}$ range corresponding to the medium-coherence region and minor variation of the high-coherence region. In this case, the lower bound $g_{synp\ min}$ of the coherence region slightly shifts to higher $g_{synp}$ values. Astrocyte-mediated facilitation of excitatory synaptic drive results in a drastic decrease of $g_{synp}$ range for the medium- and, especially, for the high-coherence regions. Further enhancement of this astrocytic influence leads to the narrowing of coherence regions. Wherein the critical value $g_{synp\ min}$ remained constant (Fig. 7).

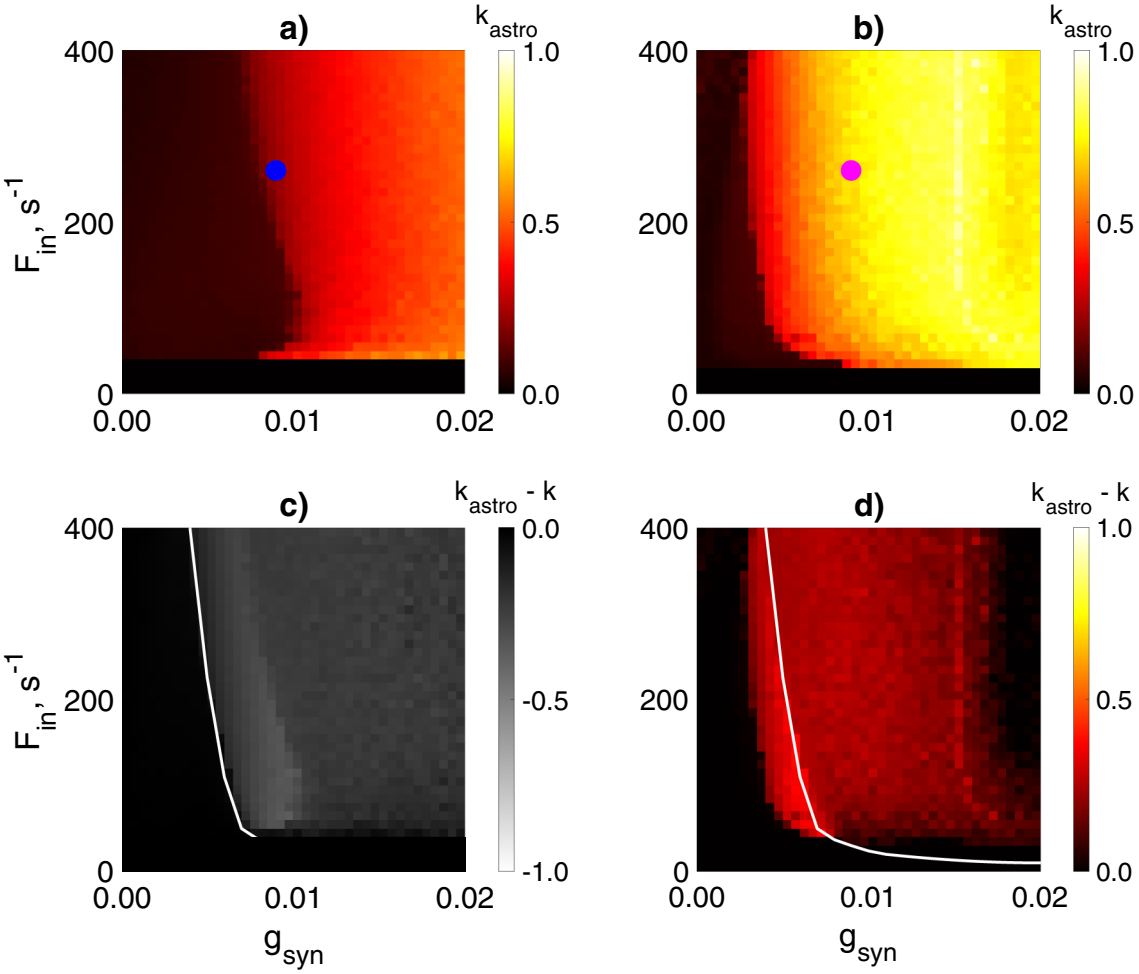


**Figure 4.** Influence of the astrocyte-induced modulation of the inhibitory synaptic transmission on the interneuron network coherence. Mean network coherence ($k_{astro}$) during astrocytic regulation of synaptic transmission is plotted against the frequency of excitatory inputs ($F_{in}$) and the synaptic weight between interneurons ($g_{syn}$) for astrocyte-mediated depression, $g_{astro} = -0.8$, (**a**) and facilitation, $g_{astro} = 1.2$, (**b**) of the inhibitory synapses. Filled circles indicate the parameter settings used in the simulations shown in Fig. 3. (**c**) Difference between (**a**) and Fig. 2c. (**d**) Difference between (**b**) and Fig. 2c. The white line corresponds to the border of the coherence region in the interneuron network without astrocyte (Fig. 2c). Each pixel represents an average of over 10 simulations. $g_{syn_P} = 0.7$ mS/cm$^2$.

Thus, pyramidal cells-astrocytes interaction can markedly enhance the coherence of oscillations in the interneuron network through the gliotransmitter-mediated decrease of excitatory synaptic drive heterogeneity. Astrocytic modulation of excitatory synaptic input can essentially improve the robustness of interneuron network $\gamma$ oscillations induced by physiologically relevant low and heterogeneous excitatory drive. In turn, astrocyte-induced potentiation of the excitatory synaptic transmission can lead to the reduction of oscillations coherence and can contribute to the impairment of $\gamma$ rhythm formation.

## Influence of the astrocytic modulation of synaptic transmission on gamma rhythm frequency in the interneuron network

The mechanisms contributing to the control of interneuron network gamma oscillations frequency are poorly understood. It is believed that they are critically dependent on the dynamics of the inhibitory synaptic conductance[7,10,11]. Computational studies indicate that frequency is regulated over a wider range by synaptic properties, tonic excitatory drive, excitation-inhibition balance, network structure, and electrical coupling[15–17]. To understand how the astrocytic modulation of synaptic transmission affects the network oscillations frequency, for two considered scenarios of neuron-astrocytic interaction, we examined the dependence of gamma oscillations frequency on the direction and magnitude of astrocytic influence (Fig. 8). The frequency of network oscillations, $F_\gamma$, was calculated only for the neural network activity with coherence $k > 0.2$, otherwise $F_\gamma = 0$. Astrocytic regulation of the inhibitory synaptic transmission in the interneuron network had only minimal effects on the network frequency (Fig. 8a). Astrocytic facilitation of the excitatory synaptic inputs to the interneurons results in a slight increase of the network oscillations frequency shifts it to the low $\gamma$ band. (Fig. 8b). Thus, astrocytic modulation of the synaptic transmission in the proposed model does not control the network frequency.

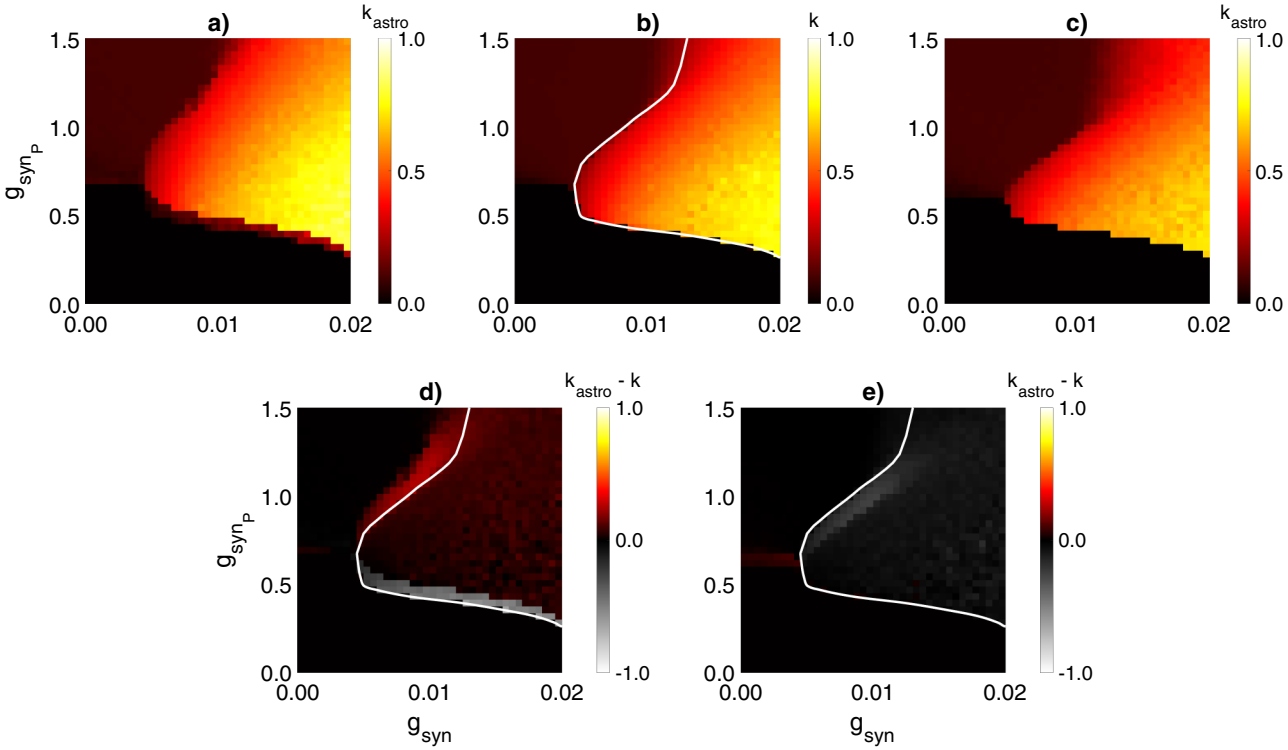


**Figure 5.** Influence of the astrocyte-induced modulation of the excitatory synaptic transmission on the interneuron network coherence. Mean network coherence, $k$, without astrocytic regulation (**b**) and during astrocytic regulation of synaptic transmission, $k_{astro}$, (**a**,**c**) is plotted against the strength of excitatory synaptic transmission ($g_{syn_P}$) and the synaptic weight between interneurons ($g_{syn}$). Astrocyte-mediated depression, $g_{astro} = -0.3$, (**a**) and facilitation, $g_{astro} = 0.3$, (**c**) of the excitatory synapses. (**d**) Difference between (**a**) and (**b**). (**e**) Difference between (**c**) and (**b**). The white line corresponds to the border of the coherence region in the interneuron network without astrocytes ($k = 0.4$). Each pixel represents an average of over 10 simulations.

## Discussion

In this study, we investigated the influence of the astrocytic modulation of synaptic transmission on the generation of synchronized oscillations in the interneuron network. Recent experimental evidence that astrocytes contribute to the cortical gamma oscillations and recognition memory[23,24] prompted us to develop a theoretical framework, which allowed us to investigate dynamical mechanisms of interplay between slow modulatory astrocytic signaling and fast synaptic transmission in formation of coherent $\gamma$ oscillations in the interneuron network. The proposed neuron-astrocyte network model incorporates the experimentally confirmed effects of astrocyte-mediated potentiation and inhibition of synaptic connection in a classical neural network model involving hippocampal interneurons (BCs) and principal neurons (pyramidal cells). The model describes the interaction of neurons and astrocytes on a network scale, at which groups of astrocytes activated by neurons form a functional dynamic network (via gap junction connectivity), and regulate the signaling of the neuronal network via the activity of gliotransmitters on synaptic connections. We found that the astrocytic regulation of signal transmission between neurons increases firing synchronicity and extends the region of coherent oscillations in biologically relevant values of the synaptic strengths. In particular, we showed that astrocyte-mediated potentiation of inhibitory synaptic transmission markedly enhances the coherence of network oscillations over a broad range of model parameters and leads to emergence of the synchronization in the interneuron network with weaker synapses. Gliotransmitter-induced depression of synaptic transmission between pyramidal cells and interneurons improves the robustness of the interneuron network gamma oscillations induced by physiologically relevant low and heterogeneous excitatory drive.

According to the in vitro experimental studies of gamma oscillations formation[10,20], tonic excitatory currents in interneurons through metabotropic glutamate receptors and kainate receptors have small amplitudes with coefficient of variation from 35%[21] to 53%[20]. Models with slow and weak synaptic connections between interneurons are able to generate oscillatory activity if heterogeneity in tonic excitatory drive is less than 3%[11]. In interneuron network models with fast and high inhibitory conductance, coherence can be achieved for the tonic excitatory drive with large amplitude and heterogeneity levels not more than 10%[12,15,22,69]. When shunting inhibition is incorporated, coherent oscillations ($k \geqslant 0.15$) can be induced by the excitatory current with low amplitude (0.5 $\mu A/cm^2$) and high heterogeneity levels (up to 70%)[17]. Under these conditions, the high-level coherence ($k \geqslant 0.5$) can be achieved for heterogeneity levels below 25% with high $g_{syn}$ values ($g_{syn} > 0.1$ $mS/cm^2$). Moreover, if Poisson trains of fast excitatory synaptic conductances with biologically relevant kinetic properties[70] are used instead of tonic excitatory currents similar to our study, the network coherence level drops below 0.4 ($k < 0.4$) for moderate heterogeneity level 10% and for $g_{syn} > 0.1$ $mS/cm^2$[17]. In our model, pyramidal neuron

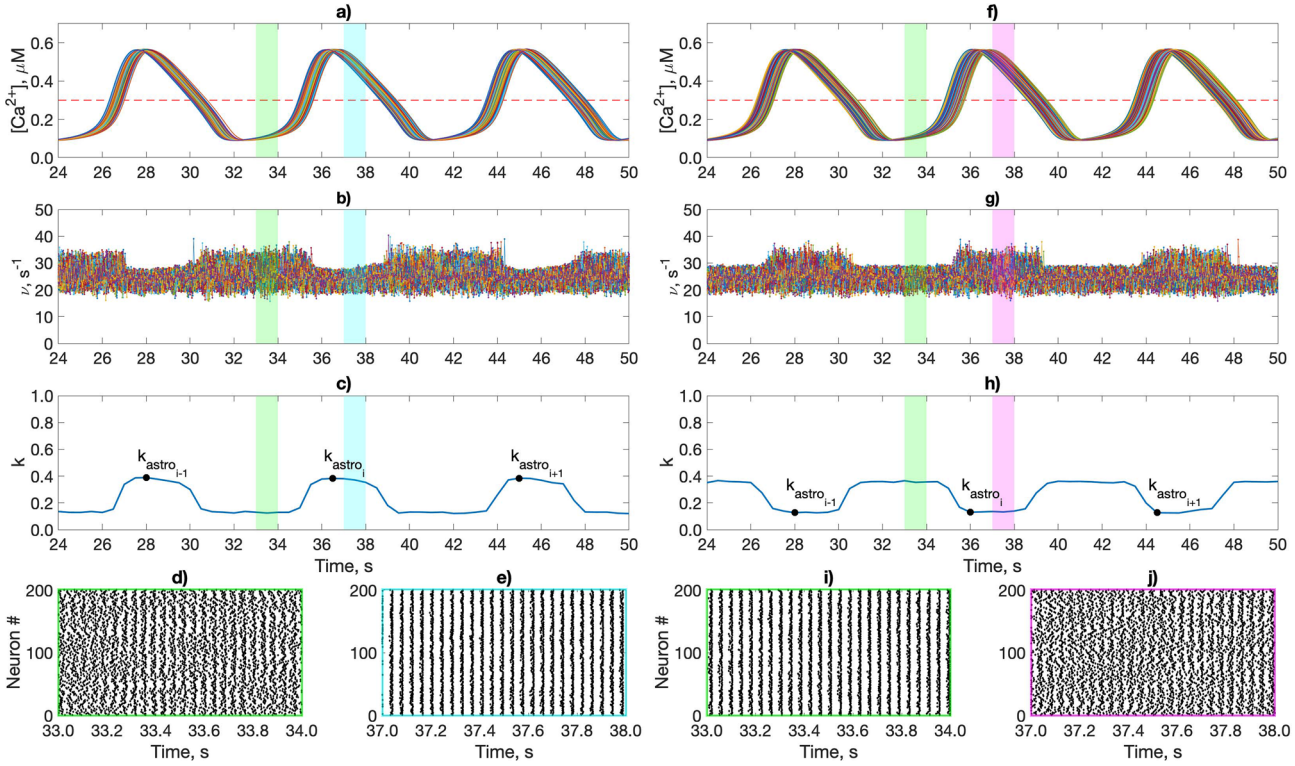


**Figure 6.** Dynamics of the astrocytic influence on $\gamma$ oscillations in the interneuron network through regulation of the excitatory synaptic drive. (**a**,**f**) The intracellular $Ca^{2+}$ concentration in the astrocytic network. (**b**,**g**) Instantaneous firing rates of interneurons. (**c**,**h**) Coherence network ($k$) dynamics. (**d**,**e**,**i**,**j**) Raster plots of an interneuron network activity. The dotted lines show the threshold $Ca^{2+}$ concentration for the astrocytic modulation of the synapse $[Ca^{2+}] = 0.3$ μM. Color coding of the 1 second long fragments of network activity: green—without astrocytic influence; blue—astrocyte-mediated depression of the excitatory synaptic transmission ($g_{astro} = -0.4$; $g_{syn_P} = 1.2$ mS/cm$^2$); magenta—astrocyte-mediated facilitation of the excitatory synaptic transmission ($g_{astro} = 0.4$; $g_{syn_P} = 0.8$ mS/cm$^2$). Minimum/maximum values of the interneurons coherence during the $Ca^{2+}$ elevations in astrocytes are marked with dots $k_{astro}$. $F_{in} = 260$ s$^{-1}$; $g_{syn} = 0.01$ mS/cm$^2$.

stimulation with Poisson trains with coefficient of variation ~ 57% for pulse amplitudes leads to the formation of heterogeneous excitatory drive received by interneuron network. These excitatory currents characterized by cell-to-cell heterogeneity levels from 25% to 45% (determined by value of $g_{syn_P}$) and low mean amplitudes (less than 0.15 μA/cm$^2$), consistent with experimental data. Here, we show that astrocyte-induced modulation of synaptic transmission helps to achieve high-level coherence ($k \geqslant 0.5$) with low $g_{syn}$ values ($g_{syn} < 0.02$ mS/cm$^2$) for such small and highly variable excitatory drive (Figs. 4b,d, 5a,d).

Although bidirectional neuron-astrocyte interaction occurs on significantly slower temporal scales (seconds to minutes) in contrast with timescales of neuronal firing and excitatory or inhibitory synaptic transmission (milliseconds), the results of this study demonstrated that astrocytes can strongly regulate the fast dynamics of neural circuits that underlie normal cognitive behavior.

Recent experimental studies provided the lines of evidence that support multifunctional astrocytic contribution to local synaptic plasticity and coordination of neural network oscillatory activity, which in turn influence the information processing (for review see[31]). Notably, both inhibitory and stimulatory effects of astrocytic modulation on the gamma oscillations are reported in the hippocampus, which is in line with the previously discussed simulation results. The optogenetic activation of ChR2-expressing astrocytes reduces the power of kainate-induced hippocampal ex vivo gamma oscillations via regulation of pyramidal cell and interneuron excitability by astrocyte-released ATP and/or adenosine[25]. The positive astrocytic influence on the gamma rhythm formation was observed in mice with genetically induced suppression of astrocytic exocytosis, which showed reduced electroencephalographic (EEG) power spectrum in the gamma frequency range in vivo and impairment of carbachol-induced gamma oscillations in vitro[23]. The activation of the astrocytic $GABA_B$ signaling triggers gliotransmission, which regulates the oscillatory activity of the neuronal network and increases the theta and gamma EEG power spectrum in vivo in mice[24]. Several studies provided direct evidence of the involvement of astrocyte signaling in cognitive functions and behavior[33,71]. However, in many of the cases, the understanding of astrocytic involvement is still incomplete. Now that we better understand the molecular components of astrocyte-neuron interactions, the new challenge is to investigate how they integrate at the network and physiological levels. To address this question, novel, bio-inspired, and detailed computational models should be developed to simulate the information processing through the coordinated activity of both astrocytes and neurons. Astrocytes

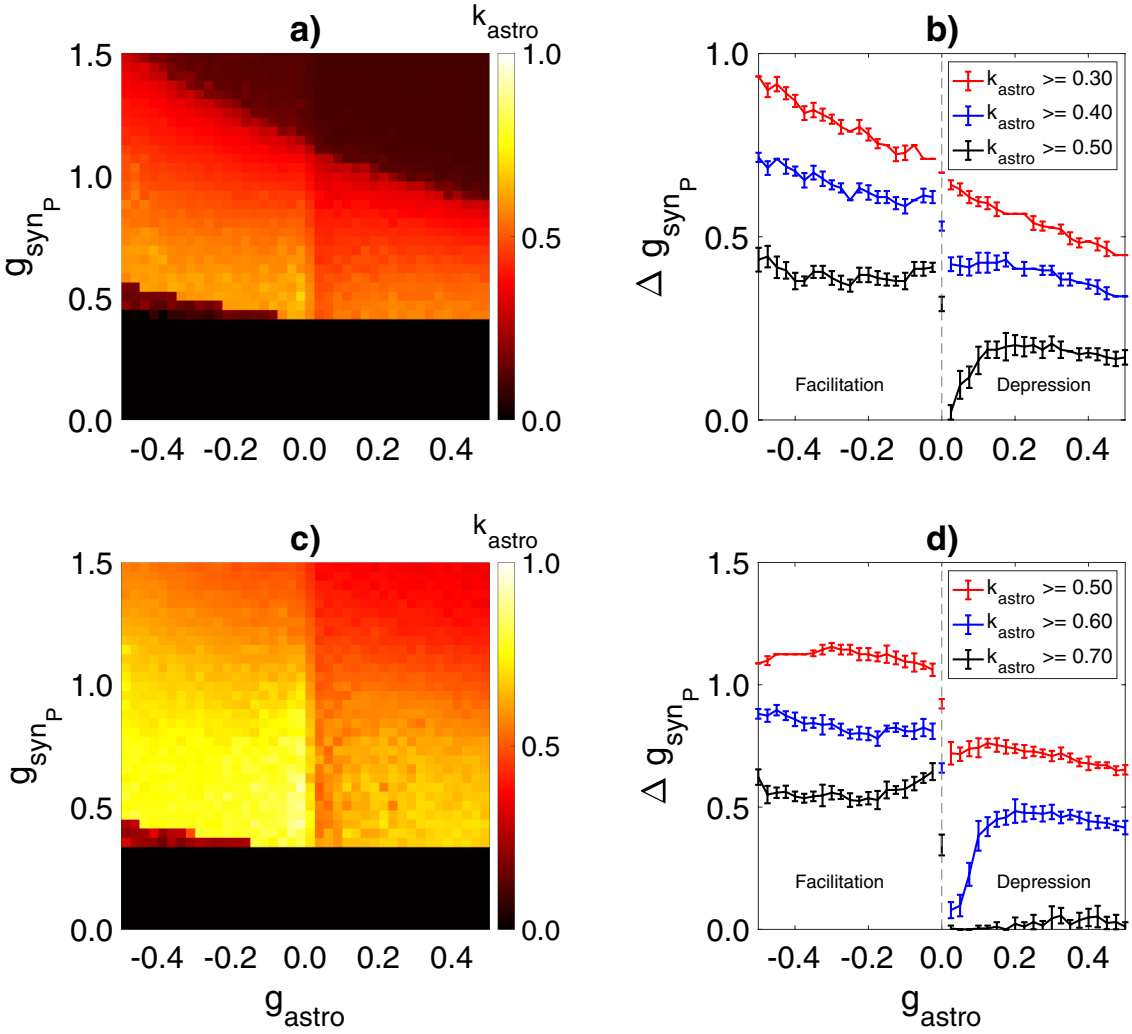


**Figure 7.** (**a**,**c**) Mean network coherence during the astrocytic regulation of synaptic transmission, $k_{astro}$, is plotted against the strength of the excitatory synaptic transmission ($g_{synp}$) and the magnitude of astrocytic modulation of the excitatory synaptic weights ($g_{astro}$). (**b**,**d**) Dependence of the $g_{synp}$ value range corresponding to the different coherence levels on the astrocytic modulation strength, $g_{astro}$. Each point represents an average ± standard deviation over 10 simulations. (**a**,**b**) $g_{syn} = 0.01\,\mathrm{mS/cm^2}$, (**c**,**d**) $g_{syn} = 0.017\,\mathrm{mS/cm^2}$.

provide an extradimensional influence over neuronal networks by a multiscale spatiotemporal integration of neural activity and can produce higher-order organization of the information coding[45]. The astrocytic $Ca^{2+}$ activity patterns could represent a guiding template that modifies the state of the local neuronal network. This modification can result in an intriguing possibility of a considerable increase of the information-possessing capacity of the mammalian brain, which could exceed the level we currently hypothesize[26].

Various computational models of the neuron-astrocyte interaction on the network level have been successfully applied to study the specific effects of neuronal activity regulation by astrocytes (for a review, see[72]). For example, Kanakov and colleagues[42] and later Abrego et al.[44] investigated the role of astrocyte-induced modulation of synaptic transmission in information processing in small neuron-astrocyte ensembles. These studies showed that the astrocytes can induce formation of the spatiotemporal activity patterns in neural network due to astrocyte-mediated facilitation of the synaptic connectivity at the timescale of astrocytic dynamics. Lenk and colleagues[35] studied the astrocytic contribution to the maintenance of the average neuronal activity level. This study showed that astrocytes could promote homeostatic regulation of the firing rate in the neuronal network similar to the influence of the extracellular matrix[73]; astrocyte-mediated modulation of synapses induces the stabilization of the neuronal activity, preventing neuronal hyperactivation. Additionally, Makovkin et al.[34] presented a two-layer oscillatory network mimics the interconnected astrocytic and neuronal networks. The astrocytic layer consists of low frequency phase oscillators coupled locally. The neuronal layer employs high frequency oscillators interconnected non-locally with regular or random topology. The analysis of the mixed coupling role in the collective dynamics and synchronization formation in such a multiplex neuron-astrocyte ensemble demonstrated that the inhibitory connections in the neural subnetwork decreases the level of phase synchronization, but sufficiently strong coupling to the astrocytes recovers synchrony in the entire network.

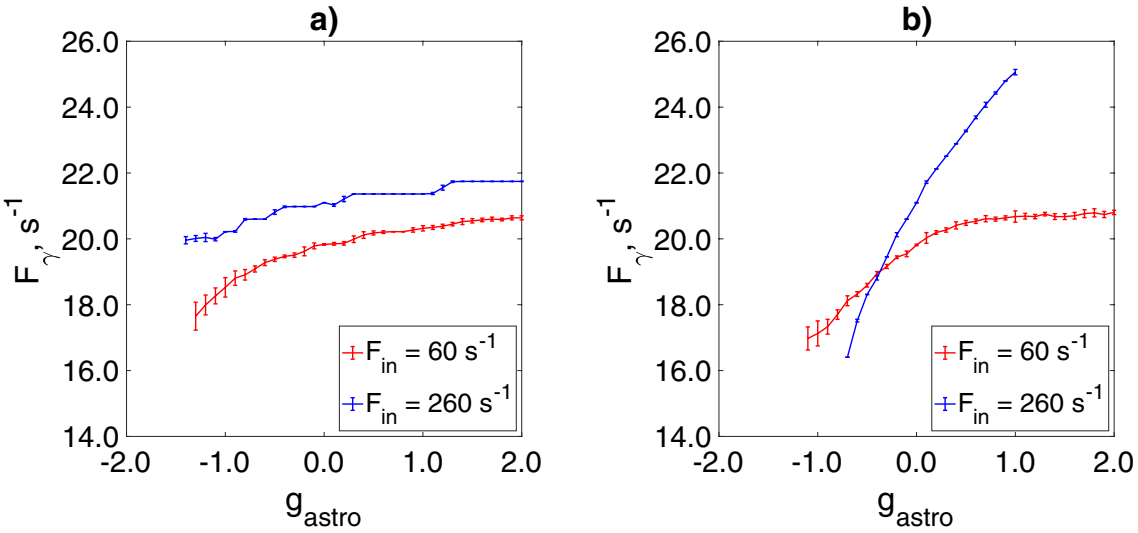


**Figure 8.** Dependencies of the network oscillations frequency on the astrocytic modulation strength, $g_{astro}$ for the astrocyte-mediated regulation of the inhibitory synaptic transmission (**a**) and of the excitatory synaptic transmission (**b**) for two different values of $F_{in}$.

Integration of astrocytic signaling in cognitive processing has implications for understanding the basis of cognitive alterations in pathological conditions. The abnormal astrocytic signaling can induce synaptic and network dysregulations leading to cognitive impairment[74–77]. Understanding the emerging role of astrocytes in regulating neural network oscillations underlying cognitive function and dysfunction opens a way for the development of novel pharmacological treatments for brain disorders.

## Code availability

The code is available at https://github.com/SpaceQuester/HodgkinHuxleyUllahJung.

Received: 21 January 2022; Accepted: 11 April 2022
Published online: 28 April 2022

## References

1. Buzsaki, G. Neuronal oscillations in cortical networks. *Science* **304**, 1926–1929. https://doi.org/10.1126/science.1099745 (2004).
2. Wang, X.-J. Neurophysiological and computational principles of cortical rhythms in cognition. *Physiol. Rev.* **90**, 1195–1268. https://doi.org/10.1152/physrev.00035.2008 (2010).
3. Cardin, J. A. *et al.* Driving fast-spiking cells induces gamma rhythm and controls sensory responses. *Nature* **459**, 663–667. https://doi.org/10.1038/nature08002 (2009).
4. Gregoriou, G. G., Gotts, S. J., Zhou, H. & Desimone, R. High-frequency, long-range coupling between prefrontal and visual cortex during attention. *Science* **324**, 1207–1210. https://doi.org/10.1126/science.1171402 (2009).
5. Fell, J. *et al.* Human memory formation is accompanied by rhinal-hippocampal coupling and decoupling. *Nat. Neurosci.* **4**, 1259–1264. https://doi.org/10.1038/nn759 (2001).
6. Lisman, J. & Idiart, M. Storage of $7 \pm 2$ short-term memories in oscillatory subcycles. *Science* **267**, 1512–1515. https://doi.org/10.1126/science.7878473 (1995).
7. Buzsáki, G. & Wang, X.-J. Mechanisms of gamma oscillations. *Annu. Revi. Neurosci.* **35**, 203–225. https://doi.org/10.1146/annurev-neuro-062111-150444 (2012).
8. Hájos, N. & Paulsen, O. Network mechanisms of gamma oscillations in the CA3 region of the hippocampus. *Neural Netw.* **22**, 1113–1119. https://doi.org/10.1016/j.neunet.2009.07.024 (2009).
9. Mann, E. O. & Mody, I. Control of hippocampal gamma oscillation frequency by tonic inhibition and excitation of interneurons. *Nat. Neurosci.* **13**, 205–212. https://doi.org/10.1038/nn.2464 (2009).
10. Whittington, M. A., Traub, R. D. & Jefferys, J. G. R. Synchronized oscillations in interneuron networks driven by metabotropic glutamate receptor activation. *Nature* **373**, 612–615. https://doi.org/10.1038/373612a0 (1995).
11. Wang, X.-J. & Buzsáki, G. Gamma oscillation by synaptic inhibition in a hippocampal interneuronal network model. *J. Neurosci.* **16**, 6402–6413. https://doi.org/10.1523/jneurosci.16-20-06402.1996 (1996).
12. Bartos, M., Vida, I., Frotscher, M., Geiger, J. R. P. & Jonas, P. Rapid signaling at inhibitory synapses in a dentate gyrus interneuron network. *J. Neurosci.* **21**, 2687–2698. https://doi.org/10.1523/jneurosci.21-08-02687.2001 (2001).
13. Penttonen, M., Kamondi, A., Acsády, L. & Buzsáki, G. Gamma frequency oscillation in the hippocampus of the rat: Intracellular analysis in vivo. *Eur. J. Neurosci.* **10**, 718–728. https://doi.org/10.1046/j.1460-9568.1998.00096.x (1998).
14. Csicsvari, J., Jamieson, B., Wise, K. D. & Buzsáki, G. Mechanisms of gamma oscillations in the hippocampus of the behaving rat. *Neuron* **37**, 311–322. https://doi.org/10.1016/s0896-6273(02)01169-8 (2003).
15. Bartos, M. *et al.* Fast synaptic inhibition promotes synchronized gamma oscillations in hippocampal interneuron networks. *Proc. Natl. Acad. Sci. USA* **99**, 13222–13227. https://doi.org/10.1073/pnas.192233099 (2002).
16. Brunel, N. & Wang, X.-J. What determines the frequency of fast network oscillations with irregular neural discharges? I. Synaptic dynamics and excitation-inhibition balance. *J. Neurophysiol.* **90**, 415–430. https://doi.org/10.1152/jn.01095.2002 (2003).
17. Vida, I., Bartos, M. & Jonas, P. Shunting inhibition improves robustness of gamma oscillations in hippocampal interneuron networks by homogenizing firing rates. *Neuron* **49**, 107–117. https://doi.org/10.1016/j.neuron.2005.11.036 (2006).

18. Andreev, A. V., Maksimenko, V. A., Pisarchik, A. N. & Hramov, A. E. Synchronization of interacted spiking neuronal networks with inhibitory coupling. *Chaos Solitons Fractals* **146**, 110812. https://doi.org/10.1016/j.chaos.2021.110812 (2021).
19. Bartos, M., Vida, I. & Jonas, P. Synaptic mechanisms of synchronized gamma oscillations in inhibitory interneuron networks. *Nat. Rev. Neurosci.* **8**, 45–56. https://doi.org/10.1038/nrn2044 (2007).
20. Fisahn, A. Distinct roles for the kainate receptor subunits GluR5 and GluR6 in kainate-induced hippocampal gamma oscillations. *J. Neurosci.* **24**, 9658–9668. https://doi.org/10.1523/jneurosci.2973-04.2004 (2004).
21. van Hooft, J. A., Giuffrida, R., Blatow, M. & Monyer, H. Differential expression of group i metabotropic glutamate receptors in functionally distinct hippocampal interneurons. *J. Neurosci.* **20**, 3544–3551. https://doi.org/10.1523/jneurosci.20-10-03544.2000 (2000).
22. Kopell, N. & Ermentrout, B. Chemical and electrical synapses perform complementary roles in the synchronization of interneuronal networks. *Proc.Natl. Acad. Sci. USA* **101**, 15482–15487. https://doi.org/10.1073/pnas.0406343101 (2004).
23. Lee, H. S. *et al.* Astrocytes contribute to gamma oscillations and recognition memory. *Proc. Natl. Acad. Sci. USA* **111**, E3343–E3352. https://doi.org/10.1073/pnas.1410893111 (2014).
24. Perea, G. *et al.* Activity-dependent switch of GABAergic inhibition into glutamatergic excitation in astrocyte-neuron networks. *eLife*https://doi.org/10.7554/elife.20362 *(2016).*
25. Tan, Z. *et al.* Glia-derived ATP inversely regulates excitability of pyramidal and CCK-positive neurons. *Nat. Commun.*https://doi.org/10.1038/ncomms13772 *(2017).*
26. Semyanov, A., Henneberger, C. & Agarwal, A. Making sense of astrocytic calcium signals: From acquisition to interpretation. *Nat. Rev. Neurosci.* **21**, 551–564. https://doi.org/10.1038/s41583-020-0361-8 (2020).
27. Araque, A. *et al.* Gliotransmitters travel in time and space. *Neuron* **81**, 728–739. https://doi.org/10.1016/j.neuron.2014.02.007 (2014).
28. Pittà, M. D., Brunel, N. & Volterra, A. Astrocytes: Orchestrating synaptic plasticity?. *Neuroscience* **323**, 43–61. https://doi.org/10.1016/j.neuroscience.2015.04.001 (2016).
29. Savtchouk, I. & Volterra, A. Gliotransmission: Beyond black-and-white. *J. Neurosci.* **38**, 14–25. https://doi.org/10.1523/jneurosci.0017-17.2017 (2018).
30. Fiacco, T. A. & McCarthy, K. D. Multiple lines of evidence indicate that gliotransmission does not occur under physiological conditions. *J. Neurosci.* **38**, 3–13. https://doi.org/10.1523/jneurosci.0016-17.2017 (2018).
31. Santello, M., Toni, N. & Volterra, A. Astrocyte function from information processing to cognition and cognitive impairment. *Nat. Neurosci.* **22**, 154–166. https://doi.org/10.1038/s41593-018-0325-8 (2019).
32. Nagai, J. *et al.* Behaviorally consequential astrocytic regulation of neural circuits. *Neuron* **109**, 576–596. https://doi.org/10.1016/j.neuron.2020.12.008 (2021).
33. Kofuji, P. & Araque, A. Astrocytes and behavior. *Annu. Rev. Neurosci.* **44**, 49–67. https://doi.org/10.1146/annurev-neuro-101920-112225 (2021).
34. Makovkin, S., Laptyeva, T., Jalan, S. & Ivanchenko, M. Synchronization in multiplex models of neuron-glial systems: Small-world topology and inhibitory coupling. *Chaos* **31**, 113111. https://doi.org/10.1063/5.0069357 (2021).
35. Lenk, K. *et al.* A computational model of interactions between neuronal and astrocytic networks: The role of astrocytes in the stability of the neuronal firing rate. *Front. Comput. Neurosci.*https://doi.org/10.3389/fncom.2019.00092 *(2020).*
36. Makovkin, S. Y., Shkerin, I. V., Gordleeva, S. Y. & Ivanchenko, M. V. Astrocyte-induced intermittent synchronization of neurons in a minimal network. *Chaos Solitons Fractals* **138**, 109951. https://doi.org/10.1016/j.chaos.2020.109951 (2020).
37. Gordleeva, S. Y., Ermolaeva, A. V., Kastalskiy, I. A. & Kazantsev, V. B. Astrocyte as spatiotemporal integrating detector of neuronal activity. *Front. Physiol.*https://doi.org/10.3389/fphys.2019.00294 *(2019).*
38. Pankratova, E. V. *et al.* Neuronal synchronization enhanced by neuron-astrocyte interaction. *Nonlinear Dyn.* **97**, 647–662. https://doi.org/10.1007/s11071-019-05004-7 (2019).
39. Gordleeva, S. Y., Lebedev, S. A., Rumyantseva, M. A. & Kazantsev, V. B. Astrocyte as a detector of synchronous events of a neural network. *JETP Lett.* **107**, 440–445. https://doi.org/10.1134/s0021364018070032 (2018).
40. Amiri, M., Hosseinmardi, N., Bahrami, F. & Janahmadi, M. Astrocyte- neuron interaction as a mechanism responsible for generation of neural synchrony: A study based on modeling and experiments. *J. Comput. Neurosci.* **34**, 489–504. https://doi.org/10.1007/s10827-012-0432-6 (2012).
41. Savtchenko, L. P. & Rusakov, D. A. Regulation of rhythm genesis by volume-limited, astroglia-like signals in neural networks. *Philos. Trans. R. Soc. B* **369**, 20130614. https://doi.org/10.1098/rstb.2013.0614 (2014).
42. Kanakov, O., Gordleeva, S., Ermolaeva, A., Jalan, S. & Zaikin, A. Astrocyte-induced positive integrated information in neuron-astrocyte ensembles. *Phys. Rev. E*https://doi.org/10.1103/physreve.99.012418 *(2019).*
43. Kanakov, O., Gordleeva, S. & Zaikin, A. Integrated information in the spiking-bursting stochastic model. *Entropy* **22**, 1334. https://doi.org/10.3390/e22121334 (2020).
44. Abrego, L., Gordleeva, S., Kanakov, O., Krivonosov, M. & Zaikin, A. Estimating integrated information in bidirectional neuron-astrocyte communication. *Phys. Rev. E*https://doi.org/10.1103/physreve.103.022410 *(2021).*
45. Nazari, S., Amiri, M., Faez, K. & Hulle, M. M. V. Information transmitted from bioinspired neuron-astrocyte network improves cortical spiking network's pattern recognition performance. *IEEE Trans. Neural Netw. Learn. Syst.* **31**, 464–474. https://doi.org/10.1109/tnnls.2019.2905003 (2020).
46. Liu, J. *et al.* Exploring self-repair in a coupled spiking astrocyte neural network. *IEEE Trans. Neural Netw. Learn. Syst.* **30**, 865–875. https://doi.org/10.1109/tnnls.2018.2854291 (2019).
47. Gordleeva, S. Y. *et al. Astrocytes Organize Associative Memory* 384–391. (Springer International Publishing, 2019). https://doi.org/10.1007/978-3-030-30425-6_45 .
48. Gordleeva, S. Y. *et al.* Modeling working memory in a spiking neuron network accompanied by astrocytes. *Front. Cell. Neurosci.*https://doi.org/10.3389/fncel.2021.631485 *(2021).*
49. Tewari, S. & Parpura, V. A possible role of astrocytes in contextual memory retrieval: An analysis obtained using a quantitative framework. *Front. Comput. Neurosci.*https://doi.org/10.3389/fncom.2013.00145 *(2013).*
50. Wade, J. J., McDaid, L. J., Harkin, J., Crunelli, V. & Kelso, J. A. S. Bidirectional coupling between astrocytes and neurons mediates learning and dynamic coordination in the brain: A multiple modeling approach. *PLoS ONE* **6**, e29445. https://doi.org/10.1371/journal.pone.0029445 (2011).
51. Tsybina, Y. *et al.* Astrocytes mediate analogous memory in a multi-layer neuron-astrocyte network. *Neural Comput. Appl.*https://doi.org/10.1007/s00521-022-06936-9 *(2022).*
52. Sik, A., Penttonen, M., Ylinen, A. & Buzsaki, G. Hippocampal CA1 interneurons: An in vivo intracellular labeling study. *J. Neurosci.* **15**, 6651–6665. https://doi.org/10.1523/jneurosci.15-10-06651.1995 (1995).
53. Halassa, M. M., Fellin, T., Takano, H., Dong, J.-H. & Haydon, P. G. Synaptic islands defined by the territory of a single astrocyte. *J. Neurosci.* **27**, 6473–6477. https://doi.org/10.1523/jneurosci.1419-07.2007 (2007).
54. Scemes, E. & Giaume, C. Astrocyte calcium waves: What they are and what they do. *Glia* **54**, 716–725. https://doi.org/10.1002/glia.20374 (2006).
55. Pawelzik, H., Hughes, D. I. & Thomson, A. M. Physiological and morphological diversity of immunocytochemically defined parvalbumin- and cholecystokinin-positive interneurones in CA1 of the adult rat hippocampus. *J. Comp. Neurol.* **443**, 346–367. https://doi.org/10.1002/cne.10118 (2002).

56. Hodgkin, A. & Huxley, A. A quantitative description of membrane current and its application to conduction and excitation in nerve. *Bull. Math. Biol.* **52**, 25–71. https://doi.org/10.1016/s0092-8240(05)80004-7 (1990).
57. Mainen, Z. F., Joerges, J., Huguenard, J. R. & Sejnowski, T. J. A model of spike initiation in neocortical pyramidal neurons. *Neuron* **15**, 1427–1439. https://doi.org/10.1016/0896-6273(95)90020-9 (1995).
58. Mainen, Z. F. & Sejnowski, T. J. Influence of dendritic structure on firing pattern in model neocortical neurons. *Nature* **382**, 363–366. https://doi.org/10.1038/382363a0 (1996).
59. Kazantsev, V. B. & Asatryan, S. Y. Bistability induces episodic spike communication by inhibitory neurons in neuronal networks. *Phys. Rev. E*https://doi.org/10.1103/physreve.84.031913 *(2011).*
60. Esir, P. M., Gordleeva, S. Y., Simonov, A. Y., Pisarchik, A. N. & Kazantsev, V. B. Conduction delays can enhance formation of up and down states in spiking neuronal networks. *Phys. Rev. E*https://doi.org/10.1103/physreve.98.052401 *(2018).*
61. Gordleeva, S. Y., Stasenko, S. V., Semyanov, A. V., Dityatev, A. E. & Kazantsev, V. B. Bi-directional astrocytic regulation of neuronal activity within a network. *Front. Comput. Neurosci.*https://doi.org/10.3389/fncom.2012.00092 *(2012).*
62. Ullah, G., Jung, P. & Cornell-Bell, A. Anti-phase calcium oscillations in astrocytes via inositol (1, 4, 5)-trisphosphate regeneration. *Cell Calcium* **39**, 197–208. https://doi.org/10.1016/j.ceca.2005.10.009 (2006).
63. Matrosov, V. *et al.* Emergence of regular and complex calcium oscillations by inositol 1, 4, 5-trisphosphate signaling in astrocytes. In *Springer Series in Computational Neuroscience* 151–176 (Springer International Publishing, 2019). https://doi.org/10.1007/978-3-030-00817-8_6.
64. Li, Y.-X. & Rinzel, J. Equations for InsP3 receptor-mediated [ca2+]i oscillations derived from a detailed kinetic model: A hodgkin-huxley like formalism. *J. Theor. Biol.* **166**, 461–473. https://doi.org/10.1006/jtbi.1994.1041 (1994).
65. Liu, Q., Xu, Q., Arcuino, G., Kang, J. & Nedergaard, M. From the cover: Astrocyte-mediated activation of neuronal kainate receptors. *Proc. Natl. Acad. Sci. USA* **101**, 3172–3177. https://doi.org/10.1073/pnas.0306731101 (2004).
66. Fellin, T. *et al.* Neuronal synchrony mediated by astrocytic glutamate through activation of extrasynaptic NMDA receptors. *Neuron* **43**, 729–743. https://doi.org/10.1016/j.neuron.2004.08.011 (2004).
67. Panatier, A. *et al.* Astrocytes are endogenous regulators of basal transmission at central synapses. *Cell* **146**, 785–798. https://doi.org/10.1016/j.cell.2011.07.022 (2011).
68. Serrano, A. GABAergic network activation of glial cells underlies hippocampal heterosynaptic depression. *J. Neurosci.* **26**, 5370–5382. https://doi.org/10.1523/jneurosci.5255-05.2006 (2006).
69. Neltner, L., Hansel, D., Mato, G. & Meunier, C. Synchrony in heterogeneous networks of spiking neurons. *Neural Comput.* **12**, 1607–1641. https://doi.org/10.1162/089976600300015286 (2000).
70. Geiger, J. R., Lübke, J., Roth, A., Frotscher, M. & Jonas, P. Submillisecond AMPA receptor-mediated signaling at a principal neuron-interneuron synapse. *Neuron* **18**, 1009–1023. https://doi.org/10.1016/s0896-6273(00)80339-6 (1997).
71. Kol, A. *et al.* Astrocytes contribute to remote memory formation by modulating hippocampal-cortical communication during learning. *Nat. Neurosci.* **23**, 1229–1239. https://doi.org/10.1038/s41593-020-0679-6 (2020).
72. Oschmann, F., Berry, H., Obermayer, K. & Lenk, K. From in silico astrocyte cell models to neuron-astrocyte network models: A review. *Brain Res. Bull.* **136**, 76–84. https://doi.org/10.1016/j.brainresbull.2017.01.027 (2018).
73. Kazantsev, V., Gordleeva, S., Stasenko, S. & Dityatev, A. A homeostatic model of neuronal firing governed by feedback signals from the extracellular matrix. *PLoS ONE* **7**, e41646. https://doi.org/10.1371/journal.pone.0041646 (2012).
74. Gordleeva, S., Kanakov, O., Ivanchenko, M., Zaikin, A. & Franceschi, C. Brain aging and garbage cleaning. *Semin. Immunopathol.* **42**, 647–665. https://doi.org/10.1007/s00281-020-00816-x (2020).
75. Whitwell, H. J. *et al.* The human body as a super network: Digital methods to analyze the propagation of aging. *Front. Aging Neurosci.*https://doi.org/10.3389/fnagi.2020.00136 *(2020).*
76. Han, J. *et al.* Acute cannabinoids impair working memory through astroglial CB1 receptor modulation of hippocampal LTD. *Cell* **148**, 1039–1050. https://doi.org/10.1016/j.cell.2012.01.037 (2012).
77. Habbas, S. *et al.* Neuroinflammatory TNFα impairs memory via astrocyte signaling. *Cell* **163**, 1730–1741. https://doi.org/10.1016/j.cell.2015.11.023 (2015).


## Acknowledgements

The work of SG was supported by the Russian Science Foundation under Grant No 21-72-10129. SM and MI thank the Ministry of Science and Higher Education of the Russian Federation Agreement No 075-15-2021-639. Numerical experiments were performed on the supercomputers Lobachevsky (University of Nizhny Novgorod), Lomonosov (Moscow State University), and MVS-10P (Joint Supercomputer Center of RAS).

## Author contributions

S.M. designed research, performed research, analyzed data, wrote the paper, E.K. performed research, M.I. designed research, wrote the paper, S.G. designed research, analyzed data, wrote the paper.

## Competing interests

The authors declare no competing interests.

## Additional information

**Supplementary Information** The online version contains supplementary material available at https://doi.org/10.1038/s41598-022-10649-3.

**Correspondence** and requests for materials should be addressed to S.M. or S.G.